The Determination of Schumann Resonance Mode Frequencies using Iterative Procedure of Complex Demodulation

Adriena ONDRÁŠKOVÁ [1], Sebastián ŠEVČÍK [1]

[1]Deparment of Astronomy, Physics of the Earth and Meteorology, Faculty of Mathematics, Physics and Informatics, Comenius University, Mlynská dolina F-1, 842 48 Bratislava, Slovak Republic; e-mail: adriena.ondraskova@fmph.uniba.sk

A b s t r a c t: The more precise determination of instantaneous peak frequency of Schumann resonance (SR) modes, especially based on relatively short signal sequences, seems to be important for detailed analysis of SR modal frequencies variations. Contrary to commonly used method of obtaining modal frequencies by Lorentzian fitting of DFT spectra, the attempt was made to employ the complex demodulation method in iterated form. The results for SR signals contaminated with low-frequency noise and hum in various degree as well as the comparison with standard method are presented. Real signals of vertical electric field component picked up at the Astronomical and Geophysical Observatory of Comenius University at Modra, Slovakia, were the primary sources.

Keywords: Schumann resonance, complex demodulation, instantaneous frequency

1. Introduction

The determination of instantaneous (short-term) modal frequencies from sample sequences of non-stationary signal consisting of several damped harmonic components (modes), plus wideband noise and hum, is not a simple task from both theoretical and computational point of view. Moreover, in the case of Schumann resonance (SR) signals, which exhibit the frequency and amplitude variations also in short-time scales (minutes and shorter) the choice of proper signal analysis method has no unique solution.

In this article, the results of iterative use of the complex demodulation (CD) method for analyzing of real Schumann resonance signals are presented.

Original (raw) signals, or signals prefiltered by band-pass digital filters were both analysed by the same method.

2. Measurements and motivation

At the Astronomical and Geophysical Observatory of Comenius University (AGO), Modra, Slovakia, the measurements of the vertical electric field component of Schumann resonances have been performed since October 2001. The experimental set-up is described in *Kostecký et al.* (*2000*) and analysis of long-term measurements in *Ondrášková et al.* (*2007, 2011*).

In (*Ondrášková et al., 2011*) the detailed analysis of daily frequency ranges (DFRs) of the first three SR modes in vertical electric field component is described. Each day was covered by 48 separate signal sequences lasting 327.68 seconds taken every half an hour (since July 2006 by 240, each taken every 6 minutes). The sampling frequency was 200 Hz. The modal frequencies were up to now determined by computing Discrete Fourier Transform (DFT) spectrum and its least-square fitting by the sum of five (or sometimes six) Lorentz functions (*Rosenberg, 2004*):

$$P(\omega) = P_0 \frac{\left(\frac{\omega_0}{\omega}\right)^2}{1 + Q^2\left(\frac{\omega}{\omega_0} - \frac{\omega_0}{\omega}\right)^2} \tag{1}$$

where P_0 stands for the peak power (for a given mode), ω_0 for the modal angular eigenfrequency and Q for the modal quality factor. This expression follows up from elementary equation of motion of the classical linear harmonic oscillator. For the spectral line profile (which has the form of the Lorentz function defined in Eq. 1), the physical meaning of the Q factor can be taken as the peak frequency of a given mode divided by the spectral line width at the half-maximum power level (full width at half-maximum, FWHM). In other words, if the oscillator (in our case the Earth–lower ionosphere resonator) is excited by a very short pulse and then leave free, its energy diminishes by a factor e^{-1} during the time $(\pi.Q/\omega)$ – the approximation valid for high values of Q.

At the first glance, this procedure seems to be quite straightforward. But a very low Q of the Earth–lower ionosphere resonance system ($Q \sim 4 \div 10$, see *Nickolaenko and Hayakawa, 2002*) results in substantial variations of "local ω_0's and Q's", which may vary from one observation site to another, because such low-Q resonator (with spatially distributed damping) cannot be treated as linear

harmonic oscillator exactly. Nevertheless, it is necessary to find (and justify) some procedure for this purpose, suitable for processing of very huge quantities of data. Extraction of modal values from signal recordings could be partially improved using non-linear fitting (*Mushtak and Williams, 2008*), but the essential shortcomings of approximation by Lorentz functions, which are the spectral functions of linear harmonic weakly damped oscillator, remain. An example of spectrum fitting by six Lorentz functions can be seen in Fig. 1.

The principal reason for our research was to determine Schumann modal eigenfrequencies by means of physically more adequate method.

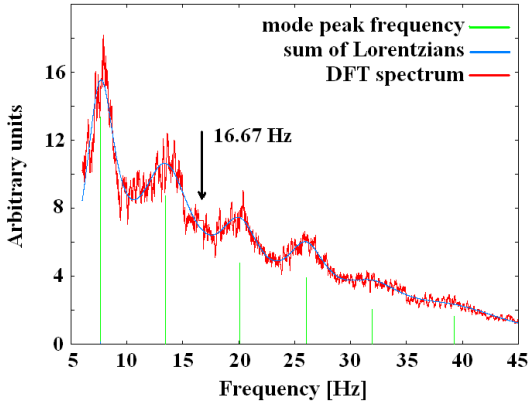

Fig. 1. An example of the sum of six Lorentz functions fitted to the power spectrum of the SR signal (the vertical electric component) from August 24, 2007, 00h 00m as determined from the whole 327.68 s long data sequence. The vertical green lines mark the position and relative amplitude of the first six eigenmodes. The peak frequencies are 7.628 13.440, 20.062, 26.006, 31.933, and 39.237 Hz. Note that the parasitic peak at 50/3 Hz is artificially cut out and the spectrum is smoothed by moving average method.

3. Methods based on direct calculations of instantaneous frequency

There is a variety of methods for determining the instantaneous (or short-term) frequency of general non-stationary process. A comprehensive and exhausting survey is given in *Boashash* (*1992*). We limit ourselves to estimation based on time derivative of continuous phase of oscillatory process (in the sense of Gabor definition based on Hilbert transformation) – (*Bingham, Godfrey, Tukey, 1967; Marple, 1989; Loughlin and Tacer, 1996; Huang et al., 2009*) and many others.

Moreover, the parametric (non-Fourier) methods, e.g. the Prony algorithm (*Fernandes et al, 2005*) are also available.

Firstly, the method of complex demodulation must be mentioned. The method of in-phase and quadrature-phase filtering (*Goodman, 1960; Verő, 1972*) was successfully applied to Schumann resonance signals in (*Sátori et al., 1996*) and in (*Sátori, 1996*). For the phase extraction only, the method of PLL (phase-locked loop) demodulation (*Gupta, 1975*) can be used, too. These methods are mathematically fully equivalent. If they are applied to "pure" input signal (free of noise and other non-harmonic wideband components), the results must be essentially the same.

The fundamental property of all methods quoted above is the determination of the time-varying phase $\varphi(t)$ of the oscillatory process in question and subsequent determination of its first time derivative $f(t)$ as

$$f(t) = -(1/2\pi)\cdot(d\varphi/dt) \tag{2}$$

The slope of $\varphi(t)$ curve indicates deviations of the instantaneous frequency around f_{est} (see also Eq. 6). The method of complex demodulation seems to be most effective and easy to implement for the analysis of signals, which (1) consist of small number ($< 10 \div 15$) even highly damped harmonic modes, (2) their frequencies are not too close one another, (3) the signal can be corrupted by noise and other wideband non-modal components.

As will be shown hereafter, the degree of noise present in signal (up to some margin) can influence only the rate of convergence if the iterative variant of complex demodulation is used.

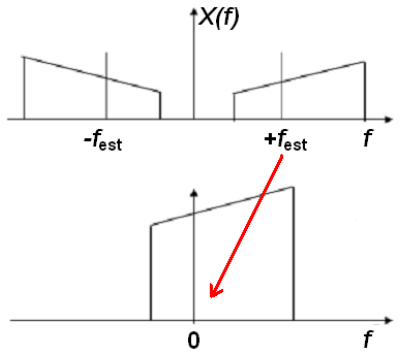

Fig. 2. The spectral "images" of original (simplified) and demodulated signal. Above is an illustrative example – the frequency spectrum of original signal. Below is the frequency spectrum of demodulated signal (before the low-pass filtering).

4. The complex demodulation method

The method of complex demodulation (*Childers and Pao, 1972; Ktonas and Papp, 1980; Sing et al., 1985; Hao et al., 1992; Myers and Orr, 1995; Gasquet and Wootton, 1997; Draganova and Popivanov, 1999*) performs several steps for extracting every modal component. However, a very crude estimate (guess) of modal frequency f_{est} must be made beforehand for each mode in question.

The CD method consists of the following steps:

a) the "preliminary filtering" or "prefiltering" of signal by a band-pass filter (relatively wide band) can enhance the contribution of the desired mode. This part of procedure is in some cases not necessary, as will be shown below;

b) the "modulation" of signal sequence $x(t)$ by a harmonic signal (cos and sin functions) of an estimated frequency f_{est}, resulting in two new sequences

$$\begin{aligned} y(t) &= x(t) \cdot \cos(\omega_{est}\, t) \\ z(t) &= x(t) \cdot \sin(\omega_{est}\, t) \end{aligned} \tag{3}$$

This and all similar operations are performed in digital domain. The frequency spectrum of the new "modulated" sequence reflects the spectrum of original signal, "folded" around the "modulation frequency" f_{est} at both sides.

c) the "demodulation" – both $y(t)$ and $z(t)$ are low-pass filtered (up to cut-off frequency f_{LP}). Low-pass filter must have phase characteristic in pass-band $< 0\ ;\ f_{LP} >$ as linear as possible. If the phase characteristics is markedly non-linear, the unwanted shift of resulting mode frequency can occur, which directly follows from Eq. (2). The resulting new sequences $\gamma(t)$ and $\xi(t)$ correspond to the original signal spectrum extracted from the frequency interval $< (f_{est} - f_{LP}); (f_{est} + f_{LP}) >$ and then shifted by f_{est} to lower frequencies (now centered around $f = 0$).
The simple graphical explanation of combined operations under b) and c) is given in Fig. 2.

d) the "computation of the instantaneous amplitude and phase residuals". Both sequences $\gamma(t)$ and $\xi(t)$ can be considered as real and imaginary components of analytic signal (complex sequence), amplitude of which is given by

$$a(t) = \left\{ \eta(t)^2 + \xi(t)^2 \right\}^{1/2} \quad (4)$$

and phase by

$$\varphi(t) = arctg \left\{ \xi(t) / \gamma(t) \right\}. \quad (5)$$

Due to previous frequency shifting, this quantity is named „phase residual".

In Eq. 5, the "unwrapped phase" or "unwrinkled phase" is necessary to compute, i.e. the function *arctg* must be corrected to phase jumps at crossings of argument between I and II, or III and IV quadrants in both directions (*Steiglitz and Dickinson, 1982; Abbas, 2005*).

e) the final step: the instantaneous frequency (in the Gabor sense) at a moment *t* is given by

$$f_0(t) = f_{est} - (1/2\pi) \cdot (d\varphi / dt)\big|_t \ . \quad (6)$$

Therefore, if the rate of phase residual in time is positive, then $f_0 < f_{est}$ and vice versa.

An example of the time graph of phase residual of the SR signal computed by CD method is given in Fig. 3.

Due to the low-pass filter, the spectrum of demodulated signals is severely limited with respect to the expected modal frequency and then with respect to sampling frequency of signal even more by relation

$f_{LP} << f_{est} << f_{sampling}$.

Therefore, the direct computation of phase residual for each signal sample will "infect" the result by numerical noise, which will be even amplified by computation of the time derivative. The possible remedy is in smoothing of computed residuals through suitable moving time window. This procedure can be considered as another low-pass filtering.

The steps a) and c) can be realized by convolution of signal sequence $x(t)$ with filter (band-pass or low-pass) unit impulse response $h(t)$, i.e. $\{x(t)*h(t)\}$ or alternatively by DFT and then by inverse DFT: computation of the signal spectrum $X(\omega) = \Phi\{x(t)\}$, then an ordinary product with filter frequency response $H(\omega)$ and, finally, the inverse DFT of such product: $\Phi^{-1}\{X(\omega).H(\omega)\}$. The symbols Φ and Φ^{-1} stand for the direct and the inverse discrete Fourier transform, respectively. Both algorithms are mathematically equivalent (taking into account that $H(\omega) = \Phi\{h(t)\}$). If the filters are prescribed by their unit impulse responses – we will show that this will be our case – the first algorithm is more advantageous in computing time, provided that time length of response $h(t)$ in use would be in reasonable limits.

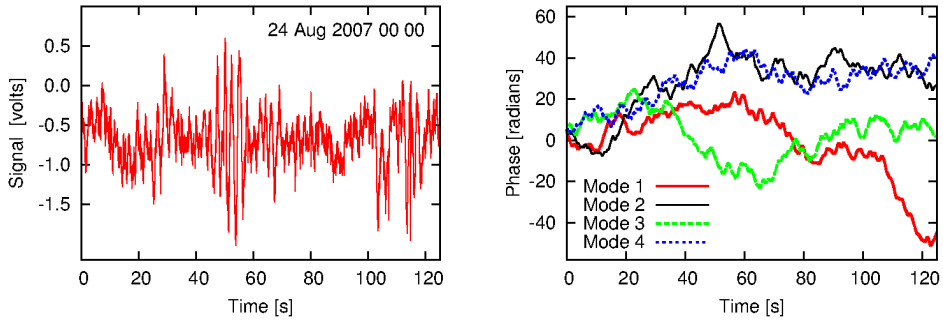

Fig. 3. (*left*) A sequence of 125 seconds of the vertical electric SR component, which is a part of a complete data block. Horizontal axis shows time in seconds, receiver output on vertical axis is in volts. (*right*): The time development of the smoothed phase residual (for the first four Schumann modes) computed by the CD method from the depicted signal. Horizontal axis is time in seconds, vertical axis in radians. The modulation frequency f_{est} = 7.80 Hz**;** the phase residual rate of +1 rad.s^{-1} corresponds to frequency deviation approx. (–0.16 Hz).

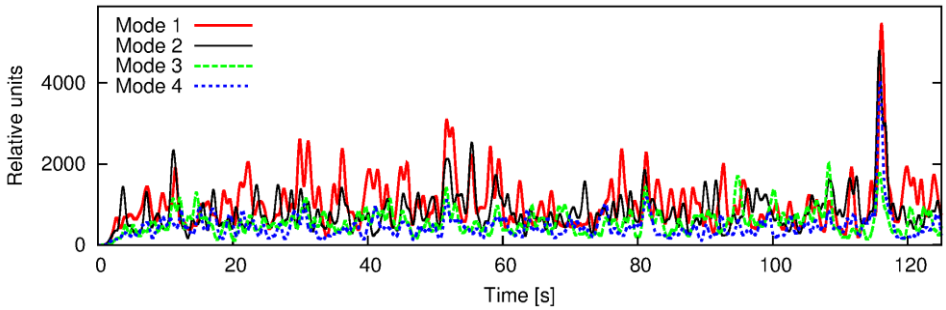

Fig 4. The smoothed amplitude residuals for the first four SR modes of the signal in Fig. 3. Horizontal axis in seconds, vertical in relative units. Smoothing was made through moving half-cosine window 2.5 s wide.

5. Amplitude residuals

The amplitude residuals can give us a look on short-time variations of instantaneous modal amplitude. In Fig. 4 we present the amplitude residuals (smoothed by 2.5 sec. moving half-cosine window) of the signal given in Fig. 3

for the first four Schumann modes. The variations of modal amplitude are clearly detectable. These variations cannot be visually attributed to variations of envelope of the unfiltered total signal, see Fig. 3.

Such second-scale amplitude variations can be observed (at filter outputs) in real time too. They can be surely attributed (*Sátori et al., 1996; Verö et al., 2000*) to short-time variations in global excitation picture of Schumann resonances – in other words, to short-time temporal and spatial variations of the global thunderstorm activity and/or the variations of the state of the lower ionospheric layers. Naturally, detection of fast modal amplitude variations (and modal amplitude variations in general) is far beyond the possibility of the traditional Lorentz functions fitting of data.

6. The iterative use of complex demodulation

The proper choice of the modulation frequency f_{est} is important for obtaining correct results. If the deviation of the modulation frequency f_{est} from the real central frequency of eigenmode peak in spectrum is too high (comparable with corner frequency of low-pass filter), then the output of low-pass filter would represent "false image" of modal line spectral contour. This represents the difficulty using the "one-shot" use of CD method. Fortunately, in case of SR signals, the coarse values of eigenmode frequencies are known (say, 7.8, 14.1, 20.6 and 26.0 Hz for the first four SR modes). Nevertheless, the possibility of more precise determination is very desirable due to their daily, seasonal and interannual variations.

Hao et al. (1992) and *Gasquet and Wootton* (*1997*) discussed the possibility of iterative use of CD procedure. The instantaneous frequency values are averaged over the complete signal sequence and subsequently this average value is taken as a new f_{est} and the complete run of complex demodulation is performed again. This may be repeated until some criterion is fulfilled, e.g. the difference in successive average frequency values, or the sum of squared frequency deviations at computation points (time samples), or simply after a prescribed number of iterations.

The key points in this method are the fact of convergence itself as well as the speed of convergence. For this reason, many examples of input signal were tested (using exclusively our own code) and in most cases the convergence was achieved in a less number of iterations than had been prescribed. Exceptions occurred only if the input signal was greatly corrupted by wideband noise (in such a degree, that even the standard procedure of Lorentz function fitting gave no satisfactory results).

7. The use of signal prefiltering

Most authors, e.g. *Hao et al.* (*1992*), *Myers and Orr* (*1994*), strongly recommend the preliminary filtering of signal before the complex demodulation is applied. If we can guess the peak frequency (f_0) of the mode to be analyzed, it is possible to employ (digital) band-pass filter centered at f_0. The choice of bandwidth remains somewhat intuitive, in some sense arbitrary.

We have used (as an experiment) the convolution filters defined in (*Verö, 1972*) and applied in (*Sátori et al., 1996*) and (*Sátori, 1996*) to Schumann resonance signals. These filters are defined by their unit impulse response. Such definition facilitates the filtering operations in the computer code, see the end of Section 4.

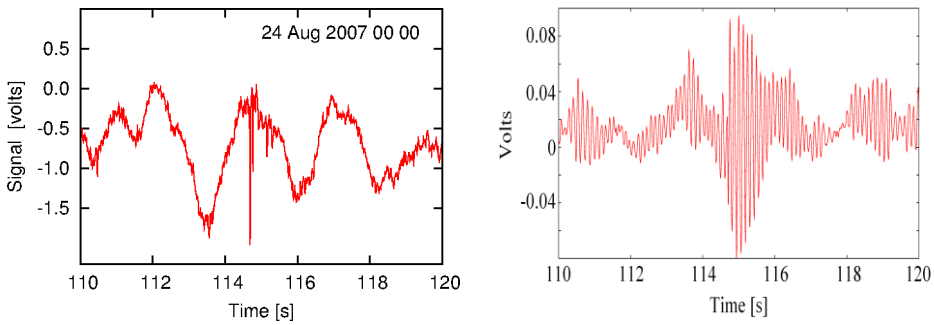

Fig. 5. (*left*) A selected part of unfiltered signal from Fig. 3 and (*right*) the same signal but prefiltered with the 1st Schumann mode filter (f_0 = 7.80 Hz). The time interval covers the signal from 110 s to 120 s after the data block beginning. Horizontal axis is in seconds, vertical axis in left graph is in volts at true receiver output. The vertical axis in the right represents the receiver output diminished by constant attenuation of the band-pass filter. Note the onset of a transient (Q-burst) at 114.67 s, which is consistent with maxima of amplitude residuals of all modes in Fig. 4.

Fig. 5 illustrates the short 10 s part of SR signal (Fig. 3) prefiltered by the 1st mode convolution filter. At 114.67 s time, the transient event (Q-burst) occurred and the approximately exponential envelope of Earth–ionosphere resonator response is clearly seen, which could give a very coarse estimate of modal quality factor Q of the resonator.

Contrary to our expectation, the use of prefilters brought only very small changes in complex demodulation results and practically no improvement in the rate of convergence in the iterative procedure of the peak frequency determination. Some exception may occur for the 1st Schumann mode, as we have confirmed by analysis of CD process applied to raw (unfiltered) and preliminary filtered signals. For the sake of brevity, we do not quote this results herein.

At the first sight, a simple comparison of the filtered (Fig. 5) and the unfiltered (Fig. 3) signal (in which no trace of harmonic component can be visible) must lead to the opposite conclusion. But – as we can see in Fig. 5 again – the modal harmonic component itself is "amplitude modulated" by chaotic (natural) signal, mostly in the frequency range ~ 0.5÷1 Hz. Such "modulation" reflects the temporal (and also spatial) variations of SR excitation by the global thunderstorm activity. The spectral profile of a modal line exhibits the permanent changes in the time scale much shorter than the length of every data block.

The complex demodulation operation is equivalent to some "implicit" band-pass filtering with passband frequencies within $< (f_{mode} - f_{LP}) ; (f_{mode} + f_{LP}) >$. Taking into account f_{LP} = ~ 0.8 Hz and about 2 Hz bandwidth of convolution prefilter, the non-efficiency of our prefiltering seems to be not very surprising. Due to these empirical facts, we did not employ the prefiltering operation in all following calculations.

The reason for slightly increased „sensitivity" of CD results in the case of the first (fundamental) Schumann mode seems to reflect the fact, that the spectral density of wideband low-frequency noise (of natural origin) has approximately $(1/f)$ character. Therefore, the fundamental (lowest frequency) mode must be the most susceptible to such noise influence.

Concerning the choice of the low-pass demodulation filter corner frequency (*Myers and Orr, 1994; Lee and Park, 1994*), a very crude estimate tends to the value about half-width of spectral line of the eigenmode under question or slightly higher. From this point of view, our choice f_{LP} ~ 0.8 Hz could be quite reasonable. It would be worth of recommendation to demodulate several signal sequences with various f_{LP} and compare the results.

8. The test results

Many computer runs were performed as test ones. In all cases, the input signals were recordings of the vertical electric field intensity in Schumann resonance band (~ 5÷100 Hz) picked up at AGO Modra, Slovakia.

The rate of convergence in the iterative use of CD was dependent on the time length of signal sequence. If this sequence was of standard duration of data block in our measurement protocol, i.e. 327.68 seconds (65536 samples), usually the criterion of average frequency change under 0.001 Hz was fulfilled after 15÷25 iterations. After splitting of data block into 16 sub-blocks (20.48 s each), the same convergence limit was achieved after 3÷5 iterations (for each sub-block alone) in most cases.

The time derivatives of phase (see Eq. 6) were computed by symmetrical five-point difference formula. In the case of full length (65536 samples) data block, the beginning and end of sequence were clamped by Hann window of 1000 samples (5 s) length, for sub-blocks (4096 samples) the width of Hann window was reduced to 100 samples (0.5 s).

The sampling frequency was in all cases 200 Hz. For demodulation, the digital 8^{th}-order Butterworth low-pass filter was used, with corner frequency 0.73 Hz, group delay in the pass-band 1.05 s, and the slope of amplitude response in the stop-band ~ 140 dB/octave.

The amplitude and phase frequency responses of the low-pass filter are given in Fig. 6.

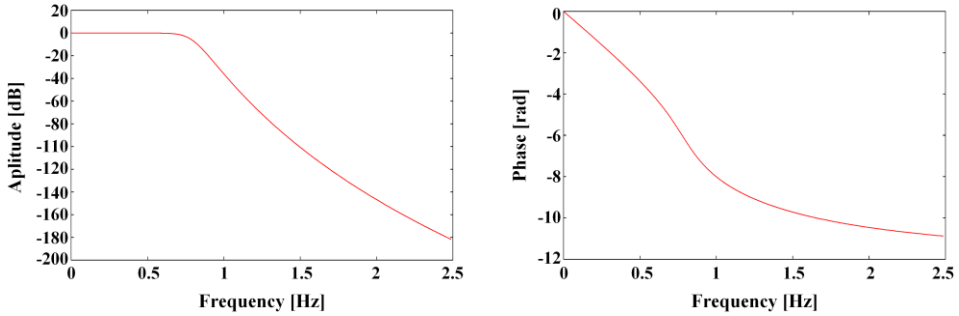

Fig 6. Amplitude (*left*) and phase (*right*) response of the low-pass demodulation filter. Horizontal axis is frequency in Hz, vertical axis is the amplitude transfer function in dB and unwrapped phase in radians, respectively.

Before processing of real Schumann signal sequences, we had executed many computations with artificial signals – amplitude and frequency modulated, like in *Draganova and Popivanov* (*1999*) – with very satisfactory results. For the sake of brevity, we do not present them here.

A very important question is the stability of the resulting computed frequency with respect to changes in f_{est} guess. In the ideal case, the result (for the same raw signal) should be independent of f_{est}. In reality, some statistically insignificant shifts in demodulation results have occurred, if the f_{est} underwent changes.

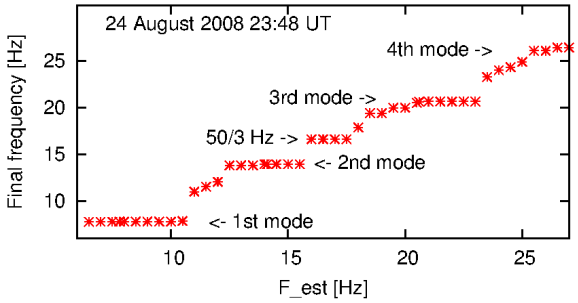

Fig. 7. The convergence graph for one complete real signal block. For a given f_{est} on the horizontal axis (stepped from 6.5 to 27.0 Hz in 0.5 Hz increments, the computed average frequency f_0 at the end of iteration is shown. Condition for termination was the difference between successive f_0's values under 0.001 Hz.

An interesting/illustrating computer experiment was made: the same real signal (complete 327.68 s long data block) was many times processed by the iterative CD code, for varying input values of f_{est} from 6.5 Hz to 27.0 Hz in 0.5 Hz increments (total 44 values). The results, i.e. the computed average frequencies are shown in Fig. 7. The "plateaus" in graph clearly coincide with Schumann resonance modal frequencies. The interval of $f_{est} < 16.0; 17.5\ \mathrm{Hz} >$ is especially worth mentioning. The iterative complex demodulation was "locked on" the parasitic component of signal at 16.67 Hz frequency (50/3). This component is often clearly visible in spectra as sharp narrow line, originating from driving frequency of electrified Austrian Railways (ÖBB), detectable at our observatory at a 55 km distance**.** The 16.67 Hz artifact is, in general, much more pronounced in magnetic field component, with significantly variable amplitude. The highest amplitude usually occurs in the second half of the night and at dawns. That is why the procedure of Lorentzian fitting has to cut out the 50/3 Hz peak (see a short horizontal line in spectrum in Fig. 1).

The rate of convergence is documented in Fig. 8. The same input signal is processed by complex demodulation twice, at first, the procedure starts from f_{est} = 7.20 Hz for the 1st mode and from 13 Hz for 2nd mode (lower curves) and

then the procedure starts from f_{est} = 8.50 Hz and 15 Hz (upper curves). Computations for the 2nd mode were terminated after the prescribed maximal number of iterations (30) in case of the upper estimate of f_{est} = 15 Hz and after 25 iterations in case of the lower estimate f_{est} = 13 Hz.

In some cases – when the input signal is grossly contaminated by noise over the whole sequence – the procedure shows no convergence and output value is slowly (and steadily) decreasing to unacceptable low values (under 1 Hz). These cases can be predicted when observing the DFT spectra of signals.

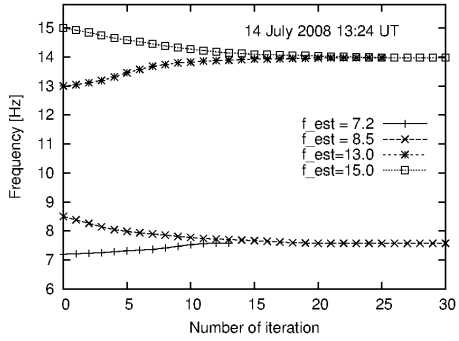

Fig. 8. The convergence graph for the 1st and 2nd Schumann resonance mode – input signal was full length block of data (327.68 s, i.e. 65536 samples).

9. Results of iterative complex demodulation

The method described above was applied to our Schumann resonance recordings. As an example, 4-day frequency variations of the first four SR modes are given in Fig. 9.

The 327.68 s long data sequences (full-length blocks) were divided into 16 sub-blocks (20.68 s long) and demodulated independently. Thus, there are 240 x 16=3840 sub-blocks per day. The complex demodulation procedure was used using 3 different termination conditions: in the first procedure only one iteration was made (results are marked green/light grey), in the second procedure run the maximal number of iterations was set 5 (red/dark grey), and in the 3rd run the maximal number of iterations was set 10 (black). This colour code is the same in all following figures. A 0.001 Hz difference of the successive values of f_0 was another termination condition, which was in many cases fulfilled earlier than maximal number of iterations. The f_{est} were set 7.8, 14.1, 20.6 and 26.0 Hz.

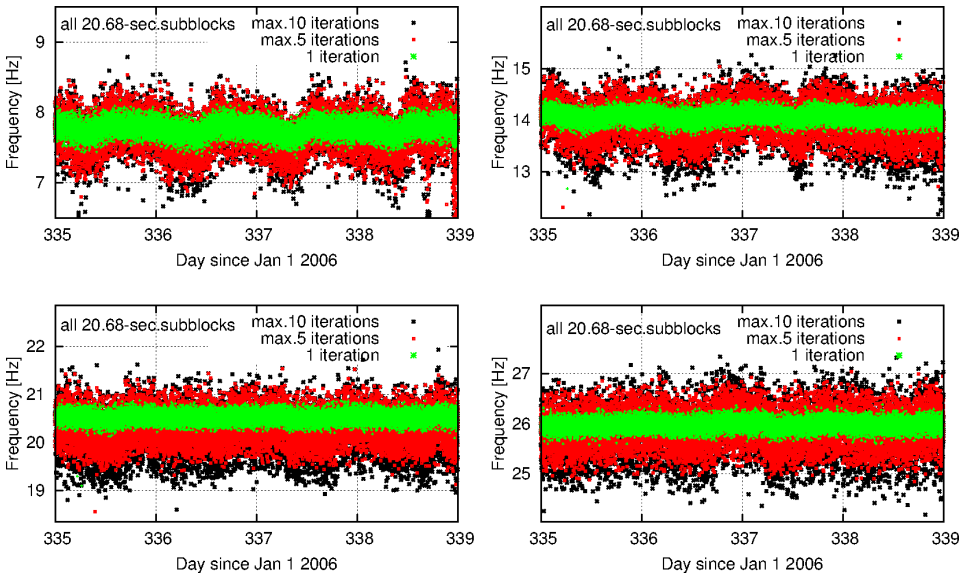

Fig 9. The results of complex demodulation of the four Schumann modes from December 1 – 4, 2006. For every day, 3840 points are given (240 data blocks each day are divided into 16 sub-blocks and every sub-block was processed independently). Points of various types and colors differentiate between demodulation procedure runs, which were limited to either 1, 5 or 10 iterations.

It can be seen that the final frequency f_0 of a sub-block after one iteration step does not differ from f_{est} by more than 0.3 Hz. A small fraction of procedure runs terminated after more than 5 iterations in which f_0 reached values below 7.2 Hz or over 8.5 Hz (for the 1st mode). The points showing significant (> 1 Hz) deviations from average frequency in most cases correspond to data sequences heavily corrupted by noise and/or technogenic hum. As a rule, neither the Lorentzian fitting gives physically plausible results at these times.

The average frequency f_0 of a complete full-length block can be easily calculated as a mean of 16 values of all 16 sub-blocks. The results using all 3 procedure runs are in Fig. 10. Naturally, these mean values are less scattered than frequencies determined for individual sub-blocks.

Finally, the results of the complex demodulation method with maximal iterations set to 10 are compared with the results of Lorentzian fitting method,

see Fig 11. As the Lorentzian fitting is applied to the full-length blocks, the black points representing the complex demodulation are means of all 16 sub-blocks (and they are the same as in Fig. 10). At the end of the 4th day, frequencies of the 1st mode decrease below reasonable value (below 7.2 Hz) what is likely caused by strong wind near the antenna site (trembling tree leaves strongly disturbed the SR signal). At these times, neither the Lorentz function fitting, nor demodulation procedure give results near the 1st mode frequency.

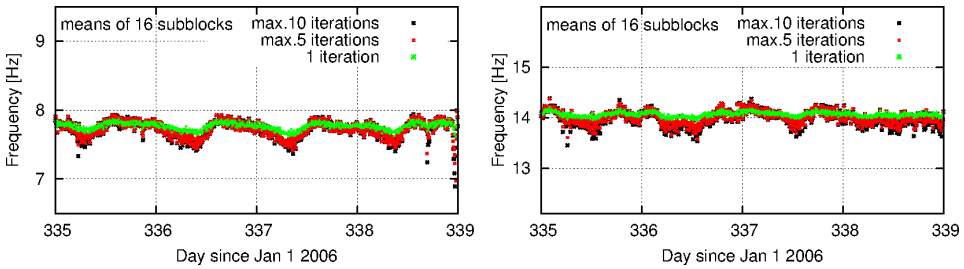

Fig. 10. Results of the 1st and 2nd mode demodulation of 327.68-second measured sequence calculated as a mean of all 16 sub-blocks. Points of different type and colors differentiate between demodulation procedure runs, which were limited to either 1, 5 or 10 iterations. The axes and the scale are the same as in Fig. 9. Naturally, these values are less scattered than frequencies determined for sub-blocks.

11. DFR derived by use of CD method

One of the most principal goals of SR analysis is the determination of average DFR's (Daily Frequency Ranges) of the SR modes for successive months of years. The DFR (for a given month) is the difference between maximal and minimal value of monthly averages taken at the same time (hour and minute). It has been shown that these quantities have direct relations to the geometrical (angular) area of the global thunderstorm foci on the Earth's surface (*Nickolaenko and Hayakawa, 2002; Ondrášková et al., 2011*). Therefore, the more precise determination of average DFR's is of great interest. The observations and also computations have justified (*Sátori et al., private communication*) that a non-negligible systematic differences exist between average monthly DFR's determined by the Lorentz function fitting of eigenmodes (traditional approach) and those computed by the complex demodulation (or possibly other non-Lorentzian) methods.

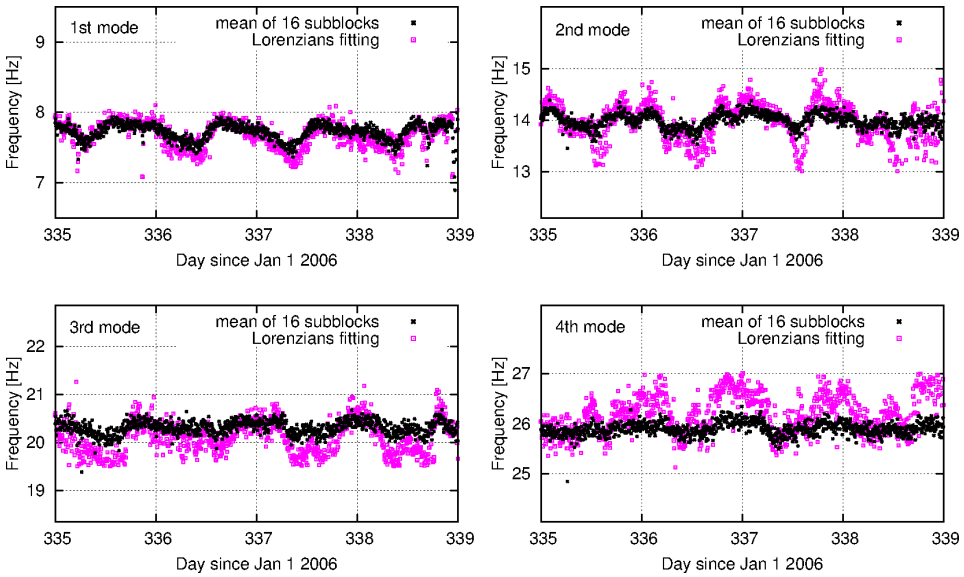

Fig. 11. Modal frequencies (black points) derived by iterative use of complex demodulation (with a limit of 10 iterations) compared with Lorentz functions fitting (violet/grey points) in the same time interval as in Fig. 9. At the end of 4th day, both methods give results below the reasonable values (below 7.2 Hz), which is likely caused by strong wind near the antenna site.

In an ideal case we have 10 data blocks per hour, therefore 240 per day multiplied by 30 (31) days, i.e. 7200 (7440) full data blocks from one particular month. The computations were made for each 20.48 s sub-block (4096 samples each), therefore for 240 x 16 = 3840 per day or 115 200 (119 040) sub-blocks per month. An average f_0 of each 7200 or 7440 blocks is calculated taking into account only physically reasonable values of f_0 of individual sub-blocks. Then a monthly mean value for a given time of day is calculated as a simple average of f_0 values from all 30 or 31 data blocks taken at the same time (hour and minute).

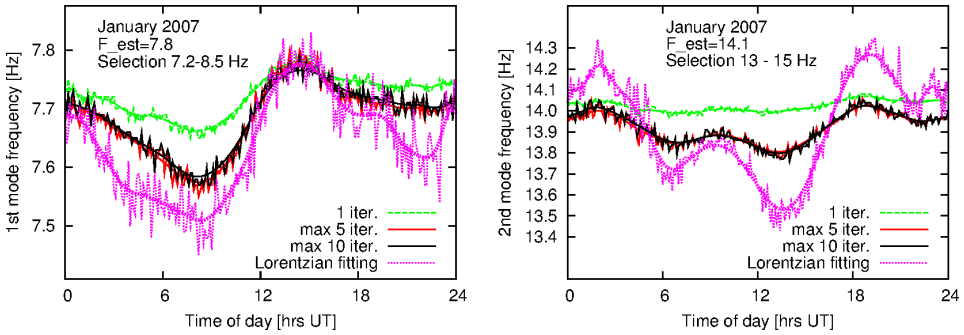

Fig. 12. Daily variations of the 1st and 2nd Schumann mode resonance frequency averaged over one month (January 2007). Individual curves show daily variation determined by complex demodulation procedures, when number of iterations was limited to 1, 5, and 10, respectively, and by the Lorentz function fitting. The initial guess value of f_{est} was taken 7.80 Hz and 14.1 Hz for the 1st and 2nd mode, respectively. Results of sub-blocks outside a reasonable interval of 7.2 – 8.5 Hz and 13 – 15 Hz have been discarded.

Daily variations of the central frequency of the 1st and 2nd SR modes obtained by the Lorentzian fitting and by the CD method can be seen in Fig. 12. It is worth mentioning that resulting f_0 after maximally 5 or 10 iterations exhibit very small differences, except the small number of cases when signal sequence was grossly contaminated by noise and the computed f_0 after 5 iterations permanently goes down to unphysical values. Occasionally, the f_0 after the 5th iteration could be still > 7.2 Hz limit (and therefore acceptable), but f_0 after final 10th iteration decreased slightly under 7.2 Hz and was discarded. Just for this reason, the curve f_0 for maximum10 iterations is for all times by a tiny value of about $0.015 \div 0.02$ Hz over the curve f_0 for maximum 5 iterations. As can be seen, the mean daily variation is less significant when results of 1 iteration are used. Using the iterative complex demodulation method, the mean daily variation as well as the DFR are comparable with those obtained by the Lorentz function fitting method in case of the 1st SR mode. But the situation is quite different for the 2nd mode (Fig. 12) – the results of Lorentz function fitting (violet/dotted curves) are much more different from complex demodulation ones (red or black curves). Moreover, the daily variation of the Lorentz fitting resembles the amplified variation of the complex demodulation results.

For typical monthly averaged DFR's for the first three Schumann resonance modes see (*Ondrášková et al., 2011*). The graphs herein were obtained by the "old" method of modal frequency computation (the fitting of

signal DFT spectra by the sum of Lorentzians). These graphs cover the interval from October 2001 (start of regular monitoring at our observatory) up to the July 2009, inclusively. The systematic lowering of modal frequencies from year to year (clearly seen in graphs therein) is in connection with the phase of solar activity cycle.

10. Conclusions

The complex demodulation method was applied to reveal frequency and amplitude variations of Schumann resonance modal spectral peaks. It was found that the iterative variant of the CD method should be used since it is less dependent on initial guess of demodulation frequency. Therefore, based on results of many computations, this method seems to be superior with respect to "one-shot" (single iteration) complex demodulation, as well as with respect to in-phase and quadrature-phase filtering method. The computation complexity of the iterative variant is practically not greater with respect to methods quoted above.

This method seems to be clearly superior compared with traditional Lorentz functions approximation. Taking into account the physical background, this method shows to be more natural approximation of the reality then traditional Lorentz functions approximation.

The iterative complex demodulation has been illustrated on processing of many real Schumann resonance signals recorded at the Astronomical and Geophysical Observatory of Comenius University in Modra, Slovakia.

An important question is how to apply CD method. There are two possibilities, either CD is applied on the whole (full-length) 327.68 s long SR records or it is applied on short sub-blocks. Results of the latter possibility are presented here. Troubles arise from records disturbed by local meteorological conditions when output of measurements or their parts are strongly saturated. Such outputs or their parts can give unphysical values of the searched central peak frequency. The approximation of SR peaks by Lorentz functions was applied on the whole 327.68 s long SR records and unreasonable values were excluded from the obtained values, e.g. only values from an interval <7.2; 8.5> were selected for the first SR mode. Partially saturated record sometimes gave reasonable values but they could contribute to the scatter of the values. The advantage of CD method applied on the short sub-blocks lies in the fact that "bad" values of the frequency from saturated sub-blocks can be discarded and the scatter of the frequency values is decreased. This may be the main reason for the differences between the monthly mean daily variations determined by the Lorentzian fitting and by the CD method applied on the sub-blocks presented

here, see Fig. 12. From this point of view, it can be concluded that CD method should be applied by iterative procedure and on the short sub-blocks evaluating each sub-block individually.

The computations by complex demodulation method were executed using our own code. On ordinary PC, the processing time for one complete day of raw data (which represents about 15.73 millions of samples) was approximately 2 hours to find all four first SR mode central peak frequencies. This time is comparable with the time spent by the Lorentzian fitting method to find modal peak frequencies, amplitudes and Q-factors of the first four SR modes.

Acknowledgements. Our sincere thanks go to the staff of AGO observatory for invaluable help in experimental arrangement. We thank also to Ladislav Rosenberg, who provided us with valuable advices and help in computer programming. The authors acknowledge the remarks to the text of this paper from Pavel Kostecký. The authors thank to the Slovak Scientific Grant Agency VEGA for financial support under the grant No. 1/0859/12.

References

Abbas K., 2005: A New Recursive Approach for Phase Unwrapping. Int. Journ. Appl. Sci. Eng., **3**, No. 2, 135–143.

Bingham C., Godfrey M. D., Tukey J. W., 1967: Modern Techniques of Power Spectrum Estimation. IEEE Trans. Audio and Electroacoustic, **AU – 15**, No. 2, 56–66.

Boashash B., 1992: Estimating and Interpreting The Instantaneous Frequency of a Signal – Part 1: Fundamentals, Proc. IEEE, **80**, No. 4 (April 1992), pp. 520–538. Part 2: Algorithms and Applications, Proc. IEEE, **80**, No. 4 (April 1992), pp. 540–568.

Childers D. G., Pao M. T., 1972: Complex Demodulation for Transient Wavelet Detection and Extraction. IEEE Trans., **AU – 20**, 295–308.

Draganova R., Popivanov D., 1999: Assessment of EEG Frequency Dynamics Using Complex Demodulation. Physiol. Res., **48**, 157–165.

Fernandes, D. A., de Almeida, L. A. L., Naidu, S. R., 2005: Prony's Method Versus FFT for Analysing Power Converter Signals. Proc. of Symp. EPE 2005, Dresden, Germany (ISBN: 90–75815–08–5), P1–P9.

Gasquet H., Wootton J., 1997: Variable–frequency complex demodulation technique for extracting amplitude and phase information. Rev. Sci. Instrum., **68**, 1111–1115.

Goodman N. R., 1960: Measuring Amplitude and Phase. J. Franklin Inst., **270**, 437–450.

Gupta S. C., 1975: Phase–Locked Loops. Proc. IEEE, **63** (2), 291–306.

Hao Y.–L., Ueda Y., Ishii N., 1992: Improved procedure of complex demodulation and application to frequency analysis of sleep spindles in EEG. Med. & Biol. Eng. & Comput., **30**, 406–412.

Huang N. E., Wu Z., Long S. R., Arnold K. C., Chen X., Blank K., 2009: On Instantaneous Frequency. Advances in Adaptive Data Analysis, **1** (2), 177–229.

Kostecký P., Ondrášková A., Rosenberg L., Turňa L'., 2000. Experimental setup for the monitoring of Schumann resonance electric and magnetic field variations at the Geophysical Observatory at Modra-Piesok. Acta Astron. et Geophys. Univ. Comenianae, **XXI–XXII**, 71–92.

Ktonas P. Y., Papp N., 1980: Instantaneous Envelope and Phase Extraction from Real Signals: Theory, Implementation and Application to EEG Analysis. Signal Processing, **2**, 373–385.

Lee J.-K., Park Y.-S., 1994: The Complex Envelope Signal and an Application to Structural Modal Parameters Estimation. Mechanical Systems and Signal Processing, **8** (2), 129–144.

Loughlin P. J., Tacer B., 1996: On the Amplitude- and Frequency-modulation Decomposition of Signals. J. Acoust. Soc. Am., Vol. 100(3), 1594–1601.

Marple S. L., 1989: A Tutorial Overview of Spectral Estimation, IEEE Trans. **SP–21**, 2152–2157.

Mushtak V.C., Williams E.W., 2008. An Improved Lorentzian Technique for Evaluating Resonance Characteristics of the Earth-Ionosphere Cavity. Atmospheric Research, doi: 10.1016/j.atmosres.2008.08.013.

Myers A.P., Orr D., 1995: ULF Wave Analysis and Complex Demodulation. Proc. of the Cluster Workshop on Data Analysis Tools, Braunschweig, Germany 28 - 30 Sept. 1994 (ESA **SP-371**, June 1995), 23–32.

Nickolaenko A. P., Hayakawa M., 2002: Resonances in the Earth–Ionosphere Cavity, Kluwer Academic Publishers, Dordrecht, 362 p.

Ondrášková A., Kostecký P., Ševčík S., Rosenberg L., 2007. Long-term observations of Schumann resonances at Modra Observatory. Radio Sci., **42**, RS2S09. doi: 10.1029/2006RS003478.

Ondrášková A., Ševčík S., Kostecký P., 2011: Decrease of Schumann resonance frequencies and changes in the effective lightning areas toward the solar cycle minimum of 2008–2009. Journal of Atmospheric and Solar-Terrestrial Physics, **73**, 534–543.

Rosenberg L., 2004: Data processing methodology of the electric and magnetic components of the Schumann resonances at Modra observatory. Acta Astron. et Geophys. Univ. Comenianae, **XXV**, 1–8.

Sing H. C., Thorne D. R., Hegge F. W., Babkoff H., 1985: Trend and Rhythm Analysis of Time-Series Data Using Complex Demodulation, Behavior Research Methods. Instruments & Computers, **17**(6), 623–629.

Sátori G., Szendrői J., Verő J., 1996: Monitoring Schumann resonances I. Methodology. J. Atmos. Terr. Phys., **58**, 1475–1481.

Sátori G., 1996: Monitoring Schumann resonances II. Daily and seasonal frequency variations. J. Atmos. Terr. Phys., **58**, 1483–1488.

Steiglitz K., Dickinson B., 1982: Phase unwrapping by factorization. IEEE Transaction on Acoustic, Speech and Signal Processing, **ASSP- 30**, No. 6, 984–991.

Verö J., 1972: On the determination of the Magneto-Telluric Impedance Tensor, Acta Geod. Geophys. Hung., **7**, No. 3–4, 333–351.

Verö J., Szendröi J., Sátori G., Zieger B., 2000: On Spectral Methods in Schumann Resonance Data Processing, Acta Geod. Geophys. Hung., **35** (2), 105–132.